

# Correlation between pathology and neuromelanin MR imaging in Parkinson's disease and dementia with Lewy bodies

Shinichiro Kitao · Eiji Matsusue · Shinya Fujii ·  
Fuminori Miyoshi · Toshio Kaminou · Shinsuke Kato ·  
Hisao Ito · Toshihide Ogawa

Received: 26 January 2013 / Accepted: 26 April 2013 / Published online: 15 May 2013  
© Springer-Verlag Berlin Heidelberg 2013

## Abstract

**Introduction** Direct correlation between neuropathological findings and postmortem neuromelanin MR imaging (NmMRI) was performed in the substantia nigra pars compacta (SNc) to clarify the pathological background of the signal changes in normal, Parkinson's disease (PD), and dementia with Lewy bodies (DLB) cases.

**Methods** NmMRI of 10 % formalin-fixed autopsied midbrains was performed in three cases (normal control, DLB, and PD) with a 3T imaging system, using a 3D gradient echo T1-weighted sequence with a magnetization transfer contrast pulse. Neuropathological examinations of the midbrains were performed, and the density of neuromelanin-positive neurons (number per square millimeter) was determined. The extent of iron deposition in the midbrain was also evaluated using ferritin immunohistochemistry. Furthermore, we directly

correlated the contrast signal ratio in the SNc and the density of neuromelanin-containing neurons.

**Results** Diffuse hyperintense areas in the SNc reflected well-preserved neuromelanin-containing neurons in the normal control case, whereas an iso-intense area in the SNc showed severe loss of neuromelanin-containing neurons in the DLB and PD cases. Increased signal intensity in the SNc was apparently not influenced by iron deposition. Furthermore, a significant positive correlation between signal intensity and the density of neuromelanin-containing neurons was seen in the SNc.

**Conclusion** Based on the direct correlation between postmortem NmMRI and neuropathological findings, signal intensity in the SNc is closely related to the quantity of neuromelanin-containing neurons but is not influenced by iron deposition.

S. Kitao (✉) · S. Fujii · F. Miyoshi · T. Kaminou · T. Ogawa  
Division of Radiology, Department of Pathophysiological  
and Therapeutic Science, Faculty of Medicine, Tottori University,  
36-1 Nishi-cho, Yonago,  
Tottori 683-8504, Japan  
e-mail: sskitao@yahoo.co.jp

E. Matsusue  
Department of Radiology, Tottori Prefectural Central Hospital,  
730 Ezu,  
Tottori, Tottori 680-0901, Japan

S. Kato  
Division of Neuropathology, Department of Brain  
and Neurosciences, Faculty of Medicine, Tottori University,  
36-1 Nishi-cho,  
Yonago, Tottori 683-8504, Japan

H. Ito  
Division of Organ Pathology, Department of Microbiology  
and Pathology, Faculty of Medicine, Tottori University,  
36-1 Nishi-cho,  
Yonago, Tottori 683-8504, Japan

**Keywords** Parkinson's disease (PD) · Dementia with Lewy bodies (DLB) · Substantia nigra pars compacta (SNc) · MRI · Neuromelanin

## Introduction

Neuromelanin is a by-product of the synthesis of monoamine neurotransmitters such as noradrenalin and dopamine and is mainly expressed in neurons of the locus coeruleus (LC) and substantia nigra pars compacta (SNc) [1–3]. Neuromelanin can induce paramagnetic T1-shortening effects when combined with metals such as iron and copper [4, 5]. T1-weighted imaging has failed to depict neuromelanin-generated contrast, presumably because of the negligible T1 difference between neuromelanin and brain tissue. Sasaki et al. reported neuromelanin-related contrast in the SNc and LC using a multislice 2D fast spin echo T1-weighted sequence with 3T MR imaging, where both the high signal-to-noise

ratio and prolonged T1 relaxation time of the brain functioned synergistically to enhance the visualization of neuromelanin-related contrast [6]. Nakane et al. [7] identified neuromelanin-generated contrast in the SNc and LC, even at 1.5 T, using a 3D gradient echo T1-weighted sequence with magnetization transfer contrast pulses, which suppress brain background signals to enhance the contrast between brain background and neuromelanin.

Parkinson's disease (PD) is characterized by severe loss of dopaminergic neurons and neuromelanin. Pathologically, dementia with Lewy bodies (DLB) closely resembles PD. Patients with DLB are characterized by the diffuse presence of Lewy bodies, cytoplasmic inclusions composed principally of alpha-synuclein, in both subcortical and cortical areas of the brain, whereas PD patients have Lewy bodies in the subcortical areas of the brain, mainly the SNc and LC [8, 9]. Sasaki et al. [6] demonstrated diminished neuromelanin levels in the SNc and LC in PD using 3T MR neuromelanin-contrast imaging. In addition, Schwarz et al. [10] suggested that T1 hyperintense area in the SNc was substantially smaller in patients with late stage PD than those with early stage PD using 3T MR neuromelanin-contrast imaging.

On neuromelanin-contrast imaging, paramagnetic T1-shortening effects of neuromelanin-containing neurons are considered to be closely related to the high signal intensity of the SNc. In addition, the iron content of the SNc is very high, approximately 20 mg/100 mg tissue, and it increases with age [11, 12]. Therefore, the possibility that a high iron concentration in the SNc may cause T1-shortening effects has been suggested in neuromelanin-contrast imaging [6].

In this study, we performed direct correlation between postmortem neuromelanin MR imaging (NmMRI) and neuropathological findings and clarified the pathological background of the signal change in normal, DLB, and PD cases. In addition, to examine the participation of iron deposition, we also evaluated the extent of iron deposition using immunohistochemistry for ferritin, which is the main storage form of iron in the brain.

## Materials and methods

We retrospectively analyzed MR brain images in three autopsy-proven cases, normal control (case 1: an 81-year-old man with normal neuropathological findings), DLB (case 2: an 81-year-old man, the modified Hoehn and Yahr Scale (H&Y) was 5, and the total score of the motor examination section of the Unified Parkinson Disease Rating Scale (UPDRS<sub>III</sub>) was 35), and PD (case 3: a 68-year-old woman, H&Y was 5, and total score of the UPDRS<sub>III</sub> was 45). After obtaining consent from the relatives, we conducted postmortem examination of these brains. All

aspects of this retrospective study were approved by the institutional review board at our institution.

Established DLB neuropathological criteria were applied [8, 9] for neuropathological diagnosis of PD and DLB. We checked for the presence of Lewy bodies with neuronal loss and gliosis in several structures including the anterior olfactory structures, lower raphe nuclei, LC, substantia nigra, amygdala, nucleus basalis of Meynert, temporal mesocortex, temporal neocortex, sensory association and premotor areas, and primary sensory and motor areas. Lewy bodies were stained using alpha-synuclein immunohistochemistry. We also checked for the presence of senile plaques and neurofibrillary tangles for Alzheimer pathology. In our cases, DLB case (case 2) showed limbic type in Lewy body type pathology and Braak stage II in Alzheimer type pathology, while PD case (case 1) showed brainstem-predominant type in Lewy body type pathology and Braak stage I in Alzheimer type pathology.

NmMRI of 10 % formalin-fixed autopsied brains (post-mortem NmMRI) was obtained in all cases using a 3T imaging system, Signa Excite HD (GE Healthcare, Milwaukee, WI, USA). First, we washed the fixed brains in running tap water for 24 consecutive hours. For gross examination, 3-mm-thick axial sections of each brain stem were obtained. The fixed 3-mm-thick sections of the upper midbrain were positioned over a surface coil 2 inches in diameter. The pulse sequences used were the T1-weighted 3D-spoiled gradient echo technique with a repetition time of 25 ms, echo time of 3.4 ms, a flip angle of 20°, field of view of 80 mm, matrix size of 384×384 (pixel size of 0.2×0.2), slice thickness of 0.8 mm, and excitation number of four times. Magnetization transfer contrast pulse was also applied. Acquisition time was 7.6 min.

For MR pathologic direct correlation, neuropathological examinations were performed in all cases using three staining methods: hematoxylin and eosin, Klüver–Barrera, and ferritin immunohistochemistry. The Klüver–Barrera method was used to evaluate myelin, and ferritin immunohistochemistry was used to reveal ferritin deposits.

Although antemortem conventional MR images such as T1-weighted and T2-weighted images were obtained, antemortem NmMRI was not obtained in all cases. However, hyperintense lesions on postmortem T1-weighted images are qualitatively well correlated with the *in vivo* imaging findings [13, 14] despite a reversal of gray/white matter contrast due to shortening of T1 and T2 relaxation times, secondary to formalin fixation [15, 16].

## Postmortem NmMRI and histological correlations in the SNc

The presence of signal changes in the SNc was evaluated on postmortem NmMRI. The signal changes in the SNc were

compared to those in the superior colliculus (SC) in each case. Also, the signal changes in the SNc were compared to the neuropathological findings, focusing on neuromelanin-containing neurons, myelinated fibers, and ferritin depositions in each case.

#### Evaluation of the signal intensity and density of neuromelanin-containing neurons in the SNc

The SNc on NmMRI in each case was divided into four parts (1: right lateral, 2: right medial, 3: left medial, 4: left lateral) (Fig. 1). The contrast ratio of each part of the SNc was measured by defining the region of interest (ROI) on a liquid crystal display following the equation:  $SS_{\text{Nc}} - SSC / SSC$ , where  $SS_{\text{Nc}}$  is the signal intensity of the SNc, and  $SSC$  is the signal intensity of the SC. ROIs were placed in the four parts of the SNc in each one of the three specimens and strictly traced according to the margins of the anatomical regions. Each size of ROI was also evaluated. All images were analyzed by two experienced neuroradiologists (S.K and E.M) and the ROIs were reproducibly measured.

The SNc on myelin-stained (Klüver–Barrera stain) sections in each case was similarly divided into four parts (Fig. 1). The number of neuromelanin-containing neurons was counted manually in each part of the SNc under a light microscope in all cases. Furthermore, to obtain density of the neuromelanin-containing neurons (number per millimeter) in each part of the SNc, the number of neurons was divided by the ROI size in each part of the SNc.

#### Statistical analysis

Furthermore, the correlation between signal intensity and density of neuromelanin-containing neurons was evaluated using linear regression analysis in all cases.

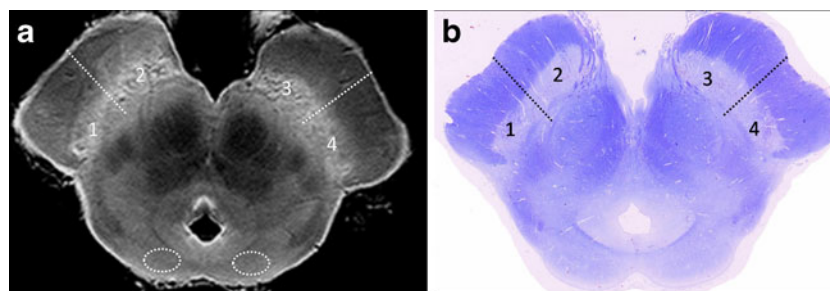


**Fig. 1** Measurement of NmMRI and myelin-stained sections. **a** Post-mortem NmMRI of the midbrain (case 1: normal control). The SNc is clearly identified as band-like hypersignal areas in the posterior portion of the cerebral peduncle. Each side of the SNc is divided into medial and lateral parts, and therefore, the SNc is divided into four parts (1: right lateral, 2: right medial, 3: left medial, 4: left lateral). Bilateral SCs are also shown (dotted lines). **b** A myelin-stained (Klüver–Barrera

## Results

### Postmortem NmMRI and histological correlations in the SNc

#### Case 1 (normal control)

Postmortem NmMRI of the midbrain showed diffuse hyperintense areas in the SNc. The signal intensity of the SNc was higher than that of the SC (Fig. 2a). Myelin staining of the SNc was the same as that of the SC, whereas strong myelin staining was seen in the red nucleus, medial lemniscus, and cerebral peduncle (Fig. 2b). Diffuse ferritin deposition in the SNc was fainter than that in the red nucleus, medial lemniscus, and cerebral peduncle (Fig. 2c). Histologically, the diffuse hyperintense area in the SNc reflected well-preserved neuromelanin-containing neurons, whereas the hyperintense area with multiple hypointense spots in the SNc reflected neuromelanin-containing neurons with bundles of myelinated nerve fibers and dilated perivascular spaces (Fig. 2d–f).

#### Case 2 (DLB)

NmMRI of the midbrain showed that the signal intensity of the SNc was the same as that of the SC. Mild hyperintensity in the left lateral part of the SNc was seen. Mild increased signal intensity was also seen in the left lateral part of the cerebral peduncle (Fig. 3a). Myelin staining of the SNc was the same as that of the SC, whereas strong myelin staining was seen in the red nucleus, medial lemniscus, and cerebral peduncle (Fig. 3b). Diffuse ferritin deposition in the SNc was milder than that in the red nucleus, medial lemniscus, and cerebral peduncle (Fig. 3c). Histologically, the signal intensity of the SNc was the same as the intensity of the SC, reflecting severe loss of neuromelanin-containing neurons, fine bundles

stain) section corresponding to **a** (case 1). The SNc is divided into four similar parts. The number of neuromelanin-containing neurons was counted in each part of the SNc in all cases. Furthermore, to obtain density of the neuromelanin-containing neurons (number per square millimeter) in each part of the SNc, the number of neurons was divided by the ROI size in each part of the SNc

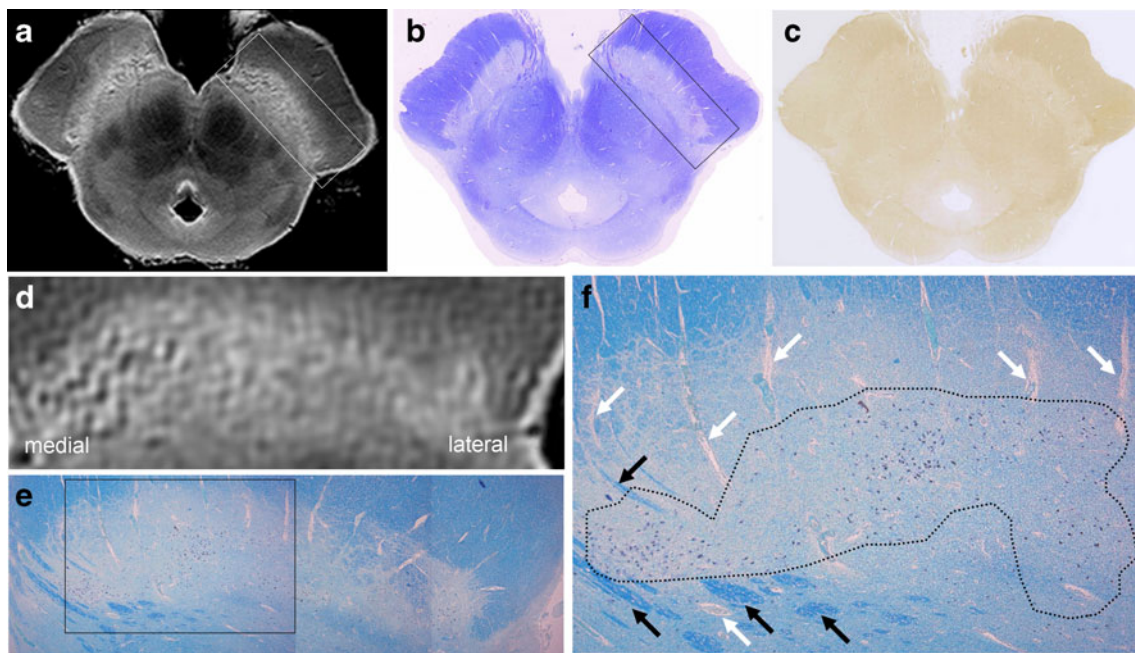


**Fig. 2** Case 1 (normal control). **a** NmMRI of the midbrain shows diffuse hyperintense areas in the SNc. The signal intensity of the SNc is higher than that of the SC. The signal intensity of the red nucleus, medial lemniscus, and cerebral peduncle is lower than that of the SC. **b** A myelin-stained (Klüver–Barrera stain) section corresponding to **a** shows that staining of the SNc is the same as that of the SC. Strong myelin staining is seen in the red nucleus, medial lemniscus, and cerebral peduncle. **c** Ferritin immunohistochemistry corresponding to **a** shows that ferritin deposition in the SNc is milder than that in the red

nucleus, medial lemniscus, and cerebral peduncle. **d** NmMRI of the SNc (boxed area in **a**) shows diffuse hyperintensity in the SNc. Multiple hypointense spots are seen in the medial side of the SNc. **e** A myelin-stained (Klüver–Barrera stain) section corresponding to the boxed area in **b**. **f** Histological finding of the boxed area in **e** shows well-preserved neuromelanin-containing neurons (dotted lines). Bundles of myelinated nerve fibers (black arrows) and dilated perivascular spaces (white arrows) are seen in the SNc

of myelinated nerve fibers, and dilated perivascular spaces (Fig. 3d–f).

### Case 3 (PD)

NmMRI of the midbrain showed that the signal intensity in the SNc was the same as that of the SC (Fig. 4a). Myelin staining of the SNc was the same as that of the SC, whereas strong myelin staining was seen in the red nucleus, medial lemniscus, and cerebral peduncle (Fig. 4b). Diffuse ferritin deposition in the SNc was milder than that in the red nucleus, medial lemniscus, and cerebral peduncle (Fig. 4c). Histologically, the signal intensity of the SNc was the same as the intensity of the SC, reflecting severe loss of neuromelanin-containing neurons, fine bundles of myelinated nerve fibers, and dilated perivascular spaces (Fig. 4d–f).

Evaluation of signal intensity and the density of neuromelanin-containing neurons in the SNc

The contrast ratios and the density of neuromelanin-containing neurons (number per square millimeter) in the four parts of the SNc in each case, for a total of 12 parts of

the SNc, are shown in Table 1. Both contrast ratios of the SNc and the density of neuromelanin-containing neurons were higher in the normal control case (case 1) than in the DLB case (case 2) and PD case (case 3). Exceptionally, in the DLB case (case 2), high contrast ratio (0.158) of the SNc and small density of neuromelanin-containing neurons (1.17) of the SNc were seen in the left lateral part (part 4). There was a significant positive correlation between signal intensity and the density of neuromelanin-containing neurons in the 12 parts of the SNc ( $\{x: \text{the density of neuromelanin-containing neurons}, y: \text{the contrast ratios of the signal intensity}\}$ ,  $y=0.000876x+0.0294$ ,  $r^2=0.382$ ,  $P<0.05$ ) (Fig. 5).

### Discussion

In this study, we directly correlated postmortem NmMRI and neuropathological findings. On the postmortem NmMRI of the midbrain, the signal intensity of the SNc was higher than that of the SC in the normal control case, whereas the signal intensity of the SNc was as same as that of the SC in the DLB and PD cases. These findings are the same as the findings with antemortem NmMRI [6]. Also, the



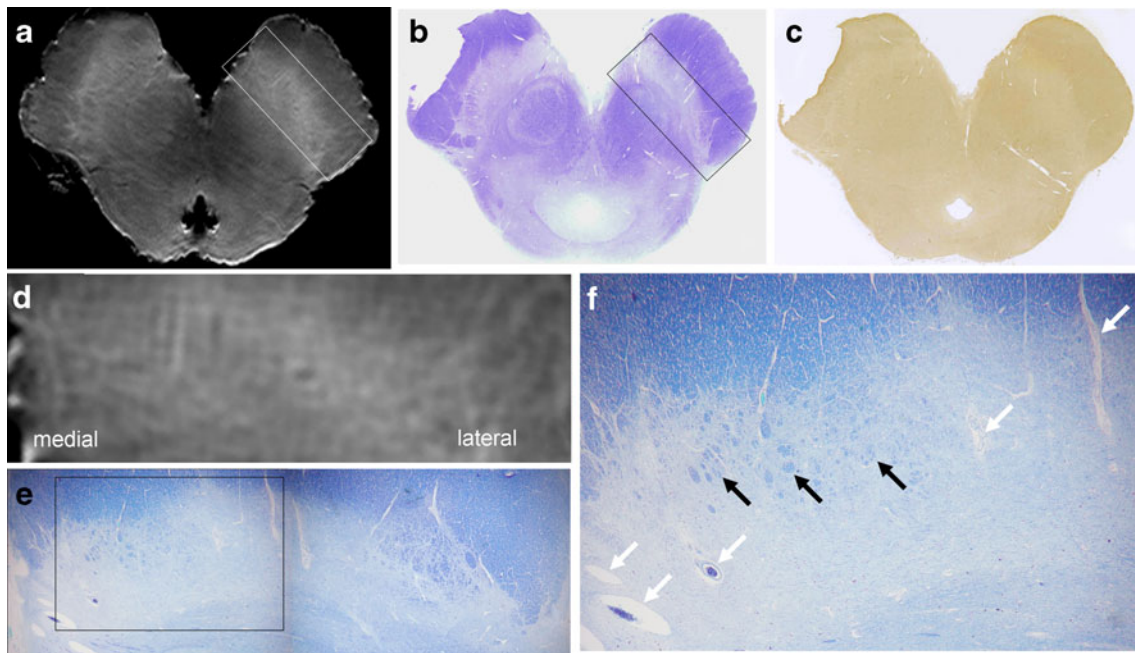


**Fig. 3** Case 2 (DLB case). **a** NmMRI of the midbrain shows no apparent hyperintense area in the SNc. The signal intensity in the SNc is the same as that of the SC. Mild hyperintensity in the left lateral part of the SNc is seen. Mild increased signal intensity is also seen in the left lateral part of the cerebral peduncle. **b** A myelin-stained (Klüver–Barrera stain) section corresponding to **a** shows that staining of the SNc is the same as that of the SC. Strong myelin staining is seen in the red nucleus, medial lemniscus, and cerebral peduncle. **c** Ferritin immunohistochemistry corresponding to **a** shows that ferritin

deposition in the SNc is milder than that in the red nucleus, medial lemniscus, and cerebral peduncle. **d** NmMRI of the SNc (*boxed area in a*) shows mild hyperintensity in the lateral part of the SNc. **e** A myelin-stained (Klüver–Barrera stain) section corresponding to the *boxed area in b*. **f** Histological finding of the *boxed area in e* shows severe loss of neuromelanin-containing neurons. Fine bundles of myelinated nerve fibers (*black arrows*) and dilated perivascular spaces (*white arrows*) are seen in the SNc

correlation between postmortem NmMRI and neuropathological findings revealed that the diffuse hyperintense areas in the SNc reflected well-preserved neuromelanin-containing neurons in the normal control case, whereas the iso-intense area in the SNc showed severe loss of neuromelanin-containing neurons in the DLB and PD cases.

In the normal control case, hyperintensity with multiple hypointense spots was seen in the SNc. Histologically, these hypointense areas reflected dilated perivascular spaces and bundles of myelinated fibers in the SNc. These structures were also seen in cases with DLB and PD. Decreased signal intensity reflecting bundles of myelinated fibers seems to be influenced by formalin fixation in postmortem T1-weighted images, a finding that is not seen in antemortem T1-weighted images. As to hypointense spot reflecting dilated perivascular spaces, the signal intensity of hypointense spots reflects water in the dilated perivascular spaces. This finding can also be seen on antemortem T1-weighted images. Therefore, preserved neuromelanin-containing neurons contribute to high signal intensity, and dilated perivascular spaces contribute to loss of signal intensity in the SNc.

We evaluated whether iron deposition contributes to high signal intensity in NmMRI. In all cases, NmMRI of the midbrain showed hypointensity in the red nucleus and white

matter such as the medial lemniscus and cerebral peduncle. Furthermore, diffuse ferritin deposition in these regions was stronger than in the SNc. Therefore, increased signal intensity in the SNc seems to not be influenced by iron deposition.

The correlation between the contrast signal ratio of each part of the SNc and the density of neuromelanin-containing neurons in the SNc was also evaluated. High contrast signal ratios were seen in the normal control case, and relatively low contrast signal ratios were seen in the DLB and PD cases. These findings seemed to reflect neuropathological changes in the SNc.

Furthermore, a significant positive correlation between the signal intensity and the density of neuromelanin-containing neurons was seen in all parts of the SNc, showing that signal intensity of the SNc is closely related to the density of neuromelanin-containing neurons.

### Limitations

There are several limitations to this study. First, we did not evaluate signal changes with iron imaging such as spin echo T2-weighted imaging, T2\*-weighted imaging, and susceptibility-weighted imaging. Instead, iron deposition

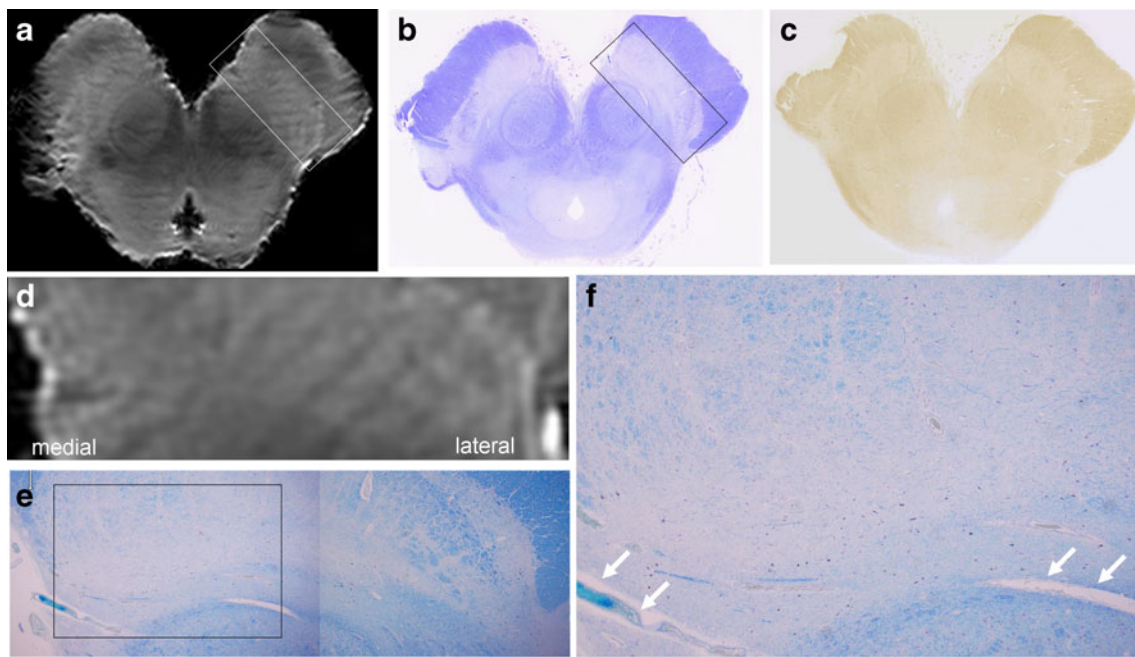


**Fig. 4** Case 3 (PD case). **a** NmMRI of the midbrain shows no apparent hyperintense area in the SNc. The signal intensity of the SNc is the same as that of the SC. Nonhomogenous hyperintensity due to artifact is seen in the right lateral part of the SNc. **b** A myelin-stained (Klüver–Barrera stain) section corresponding to **a** shows that staining of the SNc is the same as that of the SC. Strong myelin staining is seen in the red nucleus, medial lemniscus, and cerebral peduncle. **c** Ferritin immunohistochemistry

in tissue was directly evaluated using ferritin histochemistry. Iron deposition apparently did not contribute to the high signal intensity on NmMRI. Second, this study involved a small

**Table 1** The contrast ratio and the density of neuromelanin-containing neurons in each area of the SNc

	Contrast ratio of SNc	The density of neuromelanin-containing neurons
Normal control		
Part 1	0.136	9.44
Part 2	0.151	10.13
Part 3	0.104	9.46
Part 4	0.097	11.5
DLB		
Part 1	0.029	1.85
Part 2	0.020	1.66
Part 3	0.081	1.45
Part 4	0.158	1.17
PD		
Part 1	0.010	2.04
Part 2	0.001	1.31
Part 3	0.001	1.65
Part 4	0.036	2.17

SNc substantia nigra pars compacta, DLB dementia with Lewy bodies, PD Parkinson's disease

number of subjects. Third, in the DLB case (case 2), high contrast ratio of the SNc and small density of neuromelanin-containing neurons of the SNc were seen in the left lateral part (Table 1). The reason for this discrepancy remains unclear. Qualitatively, increased signal intensity was also seen not only in the left lateral part of the SNc but also in the left lateral part of the cerebral peduncle (Fig. 3). Therefore, the increased signal intensity of SNc might be influenced by artifact due to magnetic field inhomogeneities. Fourth, the LC was not evaluated in this study, although this structure is usually

corresponding to **a** shows that ferritin deposition in the SNc is milder than that in the red nucleus, medial lemniscus, and cerebral peduncle. **d** NmMRI of the SNc (boxed area in **a**) shows no apparent hyperintense area in the SNc. **e** A myelin-stained (Klüver–Barrera stain) section corresponding to the boxed area in **b**. **f** Histological finding of the boxed area in **e** shows severe loss of neuromelanin-containing neurons. Dilated perivascular spaces (white arrows) are seen in the SNc

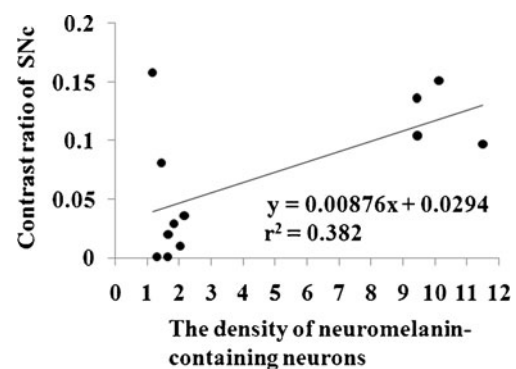


**Fig. 5** Scatter chart of the contrast ratios of the SNc determined by NmMRI and the density of neuromelanin-containing neurons (number per square millimeter) in 12 parts of the SNc ( $\{x$ : the density of neuromelanin-containing neurons,  $y$ : the contrast ratios of SNc},  $y=0.00876x+0.0294$ ,  $r^2=0.382$ ,  $P<0.05$ )

involved in PD and DLB. Despite these limitations, our results show that signal intensity in the SNc is closely related to the quantity of neuromelanin-containing neurons as shown by the direct correlation between neuromelanin imaging and neuropathological findings. As far as we know, this is the first study directly comparing postmortem NmMRI and neuropathological findings. According to the recent study by Kashihara et al. [17, 18], reduced signal changes are seen on NmMRI in the SNc not only in cases with PD, but also in cases with multiple system atrophy, progressive supranuclear palsy, and corticobasal degeneration. These findings correspond to each type of neuropathological changes. Our results provide supporting evidence for these previous results.

## Conclusion

Based on the direct correlation between NmMRI and neuropathological findings, signal intensity in the substantia nigra is closely related to the density of neuromelanin-containing neurons and is apparently not influenced by iron deposition.

**Acknowledgments** The authors would like to thank Eijirou Yamashita, Ph.D., Takuro Tanaka, BS, Naoki Iwata, BS, and Shota Sakimoto, BS, for their technical support in obtaining the high-quality MR images used in this study.

**Conflict of interest** We declare that we have no conflict of interest.

## References

- Marsden D (1965) Brain pigment and its relation to brain catecholamines. *Lancet* 10:475–76
- Graham DG (1979) On the origin and significance of neuromelanin. *Arch Pathol Lab Med* 103:359–62
- Bazelon M, Fenichel GM, Randall J (1967) Studies on neuromelanin: I. A melanin system in the human adult brainstem. *Neurology* 17:512–18
- Enochs WS, Hyslop WB, Bennett HF et al (1997) Sources of the increased longitudinal relaxation rates observed in melanotic melanoma: an in vitro study of synthetic melanins. *Invest Radiol* 24:794–804
- Enochs WS, Petherick P, Bogdanova A et al (1997) Paramagnetic metal scavenging by melanin: MR imaging. *Radiology* 204:417–23
- Sasaki M, Shibata E, Tohyama K et al (2006) Neuromelanin magnetic resonance imaging of locus ceruleus and substantia nigra in Parkinson's disease. *Neuroreport* 17:1215–8
- Nakane T, Nihashi T, Kawai H et al (2008) Visualization of neuromelanin in the substantia nigra and locus ceruleus at 1.5T using a 3D-gradient echo sequence with magnetization transfer contrast. *Magn Reson Med Sci* 7:205–10
- McKeith IG, Galasko D, Kosaka K et al (1996) Consensus guidelines for the clinical and pathologic diagnosis of dementia with Lewy bodies (DLB): report of the consortium on DLB International Workshop. *Neurology* 47:1113–24
- McKeith IG, Dickson DW, Lowe J et al (2005) Consortium on DLB: diagnosis and management of dementia with Lewy bodies: third report of the DLB consortium. *Neurology* 65:1863–72
- Schwarz ST, Rittman T et al (2011) T1-weighted MRI shows stage-dependent substantia nigra signal loss in Parkinson's disease. *Movement Disorders* 29:1633–38
- Hallgren B, Sourander P (1958) The effect of age of the non/hemin iron in the human brain. *J Neurochem* 3:41–51
- Vymazal J, Righini A, Brooks RA et al (1999) T1 and T2 in the brain of healthy subjects, patients with Parkinson disease, and patients with Parkinson disease, and patients with multiple system atrophy: relation of iron content. *Radiology* 211:489–95
- Kinoshita T, Ogawa T, Yoshida Y et al (2005) Curvilinear T1 hyperintense lesions representing cortical necrosis after cerebral infarction. *Neuroradiology* 47:647–51
- Castillo M, Scatliff JH, Kwock L et al (1996) Postmortem MR imaging of lobar cerebral infarction with pathologic and in vivo correlation. *Radiographics* 16:241–50
- van den Hauwe L, Parizel PM, Martin JJ et al (1995) Postmortem MRI of the brain with neuropathological correlation. *Neuroradiology* 37:343–9
- Tovi M, Ericsson A (1992) Measurements of T1 and T2 over time in formalin-fixed human whole-brain specimens. *Acta Radiol* 33:400–4
- Kashihara K, Shinya T, Higaki F (2011) Neuromelanin magnetic resonance imaging of nigral volume loss in patients with Parkinson's disease. *J Clin Neurosci* 18:1093–6
- Kashihara K, Shinya T, Higaki F (2011) Reduction of neuromelanin-positive nigral volume in patients with MSA, PSP and CBD. *Intern Med* 50:1683–7